S0021-9797(04)00355-8/FLA AID:10153 Vol.●●●(●●●)
ELSGMLTM(YJCIS):m5 2004/04/06 Prn:9/04/2004; 15:00

yjcis10153

P.1 (1-15)
by:R.M. p. 1

Available online at www.sciencedirect.com

SCIENCE DIRECT®

Journal of Colloid and Interface Science ●●● (●●●●) ●●●–●●●

JOURNAL OF
Colloid and
Interface Science

www.elsevier.com/locate/jcis

Nonlinear electrokinetics and "superfast" electrophoresis

Yuxing Ben, Eugene A. Demekhin, and Hsueh-Chia Chang *

Department of Chemical and Biomolecular Engineering, University of Notre Dame, Notre Dame, IN 46556, USA

Received 23 September 2003; accepted 1 April 2004

Abstract

Nonlinear and nonequilibrium electrophoresis of spherical particles of radius a is shown to be possible when the solid surface allows field or current penetration. At low particle Peclet numbers, transient capacitative charging occurs until the surface polarization completely screens the external field. For a DC applied field E_∞, the resulting electrokinetic velocity reaches Dukhin's maximum value of $\hat{\epsilon}E_\infty^2 a/\mu$, where $\hat{\epsilon}$ and μ are the liquid permittivity and viscosity. At high Peclet numbers, electroosmotic convection of the electroneutral bulk stops the transient charging before complete field-line exclusion. For an ion-selective and conducting spherical granule, the polarization is then determined by the steady-state Ohmic current driven by the penetrated external field. The high-Peclet electrokinetic velocity is lower, diffusivity-dependent and scales as $E_\infty^{2/3}a^{1/3}$.

Keywords: Nonlinear electrophoresis; Ion exchange; Nonlinear slip velocity; Diffusion layer

1. Introduction

There is considerable interest in using electrokinetics to move fluids, separate bioparticles and identify bacteria in the new field of microfluidics [1]. We will analyze a unique class of electrokinetics that can be called nonequilibrium or nonlinear electrokinetics. However, to better contrast this class of electrokinetic phenomena with traditional linear and equilibrium electrokinetics, we first review some basic premises in electrokinetics that are often omitted but must be rescrutinized and reformulated for nonlinear electrokinetics (for an excellent treatment, see [2]). These premises concern transition of the potential from the polarized region to the external bulk.

1.1. Linear equilibrium electrokinetics

The Maxwell force per unit volume applied by an external field E_∞ on a body with mobile charge density $\rho = C^+ - C^-$, where $C^\pm$ are the cation and anion concentrations, is ρE_∞ in vectorial form. Polarized regions with a net charge ρ and a finite Maxwell force occur near dielectric surfaces with bound surface charges. These bound charges are almost solely responsible for a large normal surface electric field $E_s = q_s/\hat{\epsilon}$, where q_s is the surface charge density and $\hat{\epsilon}$ the dielectric constant (permittivity) of the electrolyte.

The electrostatic force exerted by E_s rapidly attracts surrounding counterions such as cations even in the presence of the external applied field E_∞, viz. $E_s \gg E_\infty$. If the surface is impenetrable to ions (it does not allow current flux), the counterions quickly form an equilibrium Boltzmann distribution $C^+(y) = C_\infty \exp(-z^+\Delta\phi/(RT/F))$, where C_∞ is the bulk electrolyte concentration, such that its electromigration inward flux is balanced exactly by outward diffusive flux, resulting in no net flux. The potential difference $\Delta\phi(y) = \phi(y) - \phi(\infty)$ is relative to the bulk at $y = \infty$. The co-ions have a similar Boltzmann distribution $C^- = C_\infty \exp(z^-\Delta\phi/(RT/F))$. However, due to the opposite electrostatic driving force on each, there is an excess of counterions and a deficit of co-ions near the surface—there is polarization (see schematic in Fig. 1).

The thickness of this polarized Debye layer $\lambda = \sqrt{RT\hat{\epsilon}/F^2C_\infty}$, for an electrolyte of concentration C_∞, ranges from 10 to 100 nm. Outside the Debye layer, E_s approaches zero and the potential difference $\Delta\phi$ approaches zero at large y, $\Delta\phi(y \to \infty) = 0$. The overall potential drop $\Delta\phi(0)$ is called the zeta potential ζ and for $\zeta/(RT/F) \ll 1$, it is of $O(E_s\lambda)$.

The condition $(E_\infty/E_s) \ll 1$ also stipulates an absence of external field penetration into the Debye layer. A simple

* Corresponding author. Fax: +1-574-631-8366.
E-mail address: hchang@nd.edu (H.-C. Chang).
URL: http://www.nd.edu/~changlab.

0021-9797/$ – see front matter © 2004 Published by Elsevier Inc.
doi:10.1016/j.jcis.2004.04.004

S0021-9797(04)00355-8/FLA AID:10153 Vol.●●●(●●●)
ELSGMLTM(YJCIS):m5 2004/04/06 Prn:9/04/2004; 15:00
yjcis10153
P.2(1-15)
by:R.M. p. 2

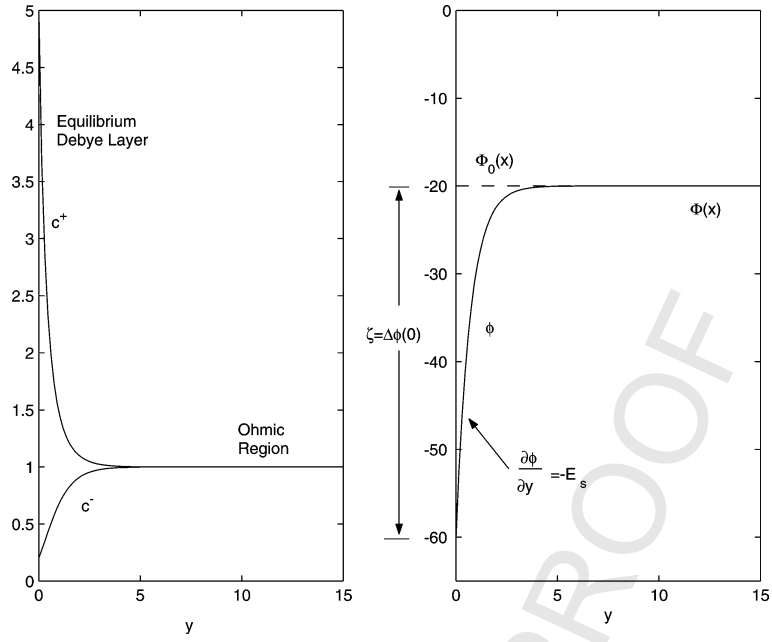

Fig. 1. Numerical solutions of the equilibrium concentration and potential profiles. The parameter are $\epsilon = 0.07$ and $C_s^+ = 5$. The potential drop $\Delta\phi(0)$ is uniform.

application of Gauss divergence theorem then shows that total charge in the Debye layer is equal to the number of bound charge. Two equal numbers of opposite charges, one bound to the surface and one confined to the thin Debye layer, are separated by an average distance of λ to form a molecular capacitor of enormous capacitance.

Most importantly, the total Maxwell force, which only exists in the polarized Debye layer, is controlled by the net charge within the Debye layer, which is equal to the total bound surface charge. The surface charge hence controls the electrokinetic velocity of surfaces with equilibrium Debye layers, known as the Smoluchowski velocity [2]

$$U_s = -\frac{\hat{\epsilon}\Delta\phi(0)E_\infty}{\mu} = -\frac{\hat{\epsilon}\zeta E_\infty}{\mu}, \tag{1}$$

where $\zeta \sim O(E_s\lambda)$ and $E_s = q_s/\hat{\epsilon}$. This equilibrium slip velocity is linear with respect to the applied field E_∞ and the related phenomena are termed linear electrokinetics. Since the Maxwell force is confined to the Debye layer, this slip velocity is independent of any macroscopic length scales—it only depends on the Debye layer thickness, $\zeta \sim O(E_s\lambda)$.

In fact, these linear electrokinetic phenomena, due to equilibrium ion distributions established by a large surface field, have many interesting features. With uniform surface charge and zeta potential and without applied pressure gradient, the applied field lines are identical to the stream lines [3]. As the external potential in the electroneutral Ohmic bulk region obeys the Laplace equation, the flow becomes a potential flow without vorticity and viscous shear even in the smallest channels. Significant Maxwell stress obviously exists in the Debye layer and this potential flow hence refers to the region outside the Debye layer. This similarity between field and stream lines is the major obstacle to transporting bubbles electrokinetically [4]. In fact, due to the invariance to macroscopic scales, the slip velocity (1) is identical for particles of arbitrary size and shape [3,5] and these particles do not interact as long as their surface charges are the same. These features have many advantages and disadvantages in microfluidic applications. The lack of shear minimizes Taylor dispersion [6] but its irrotational character implies that mixing vortices cannot be created electrokinetically. Noninteracting particles do not aggregate readily but are also difficult to separate and capture. The linearity of the slip velocity with respect to the electric field limits its magnitude to less than 1 mm/s [7] for realistic DC applied fields of less than 100 V/cm.

1.2. AC nonlinear and nonequilibrium electrokinetics

Due to the mentioned disadvantages, there is considerable interest to violate some of the mechanisms that lead to linear and irrotational electroosmotic flow. A large family of nonlinear and nonequilibrium electrokinetic phenomena have been found or rediscovered recently. All of them work under the same basic principle—to induce nonuniform polarization within the double layer with the external field or with the electromigration it drives. The normal external field must be significant compared to surface field E_s within the double layer for these phenomena to occur. As a result, the Debye layer polarization is dependent on the normal external field, as well as the surface field due to surface charges. In fact, this external-field-induced polarization should be largest if there is no surface charge. In particular, a constant-potential surface (a high permittivity dielectric, a metal or a conducting granule) that allows maximum field or current penetration would enhance this new polarization phenom-

enon. If the surface has a curvature such that the normal external field is not uniform on its surface or if the external field is by itself nonuniform, the polarization would also be nonuniform. As a result, there is a tangential gradient in the slip velocity and a tangential velocity gradient (shear rate) appears to revoke the stress-free irrotational character of uniform polarization. More over, since the polarization is external field dependent, the potential drop $\Delta\phi(0)$ across the polarized layer should be field dependent. A direct generalization of (1) suggest the resulting electroosmotic and electrophoretic velocities should depend nonlinearly on the external field. We hence expect a much larger velocity than linear electrokinetics at large fields. If nonlinear electrokinetics is produced by current penetration with a constant ion flux, equilibrium ion distributions can no longer exist. These nonlinear electrokinetic phenomena are hence often nonequilibrium in nature.

Another interesting feature of nonlinear electrokinetics occurs for the Maxwell stress induced by an AC field. If the dynamic polarization is due entirely to the normal field and is fast compared to the period of the AC field [8], the Maxwell stress is always in the same direction and has a nonzero time average. Both the charge density ρ due to polarization and the field E_∞ alternate in sign in phase such that the Maxwell force ρE_∞ retains the same sign. Hence, nonlinear AC electrokinetics tends to produce very fast velocities at large fields. At sufficiently high frequencies, AC currents do not penetrate biological cells and electron-transfer or dissolution electrode reactions that produce undesirable bubbles/contaminants are also absent. One can hence profitably employ high-field AC electrokinetics in microfluidic devices more than DC electrokinetics [8–10].

A corollary of this observation is that equilibrium linear electrokinetic phenomena do not exist for an AC external field. From (1), since the zeta potential is specified by the surface charge and is time independent and since the time-average of the applied field E_∞ vanishes exactly for an AC field, time-average U_s is exactly zero for linear AC electrokinetics whose polarization is determined by surface charges.

Because field-induced polarization requires external field penetration, the total charge within the polarized layer is no longer equal to the total surface charge. For a constant potential surface (corresponding to a metal or a conducting granule), every ion that is driven into the polarized layer by the external field will be compensated by an opposite charge that moves even more rapidly to the surface on the solid side. This compensation would ensure there is no net charge on two sides of the surface and the potential remains the same. However, the number of ions that can be driven into the polarized layer can, in principle, be increased arbitrarily by raising the applied field. This field-dependent polarization accounts for the nonlinear dependence of the electrokinetic velocity on the applied field E_∞.

The situation is more complex with insulated boundaries. It is not clear whether such field-induced polarization is possible for insulated boundaries in the limit of $(\lambda/a) \ll 1$, where a is the radius of the spherical granule. Nevertheless, if it is possible, the polarization would not be specified by the surface charge and field.

The most commonly known nonlinear electrokinetic phenomenon is AC dielectrophoresis where charging and discharging of the double layer by the external fields leads to external-field-induced dipoles in dielectric particles. The dielectrophoretic velocity is proportional to the divergence of the square of the electric field intensity and is hence clearly nonlinear. The charging by the external field in dielectrophoresis are often modeled as a resistor and capacitor in parallel [9] and is sometimes known as the Maxwell–Wagner effect. However, detailed analysis of the actual double layer charging in dielectrophoresis is still lacking. The mathematical difficulty lies in the insulated boundary condition, as we shall examine subsequently.

Another kind of nonlinear electrokinetic phenomenon occurs at electrodes supplying a high-frequency AC field. The frequency is usually beyond hundreds of kHz such that Faradaic reactions do not occur at the electrodes. Consequently, ions are charged and discharged by the external field as in dielectrophoresis. This polarization leads to strong electroosmotic vortices on the electrodes or constant-potential surfaces that have been observed and analyzed [8,10,11]. The vortices dramatically demonstrate that linear electroosmotic potential flow has been revoked. Unlike dielectrophoresis, the constant potential surface condition allows matching with the external field to resolve the all-important external field penetration. Also, the dynamic charging and discharging of ions into the double layer by the external AC field yields an interesting dynamic screening phenomenon that develops over a time scale of $\lambda a/D^+$ [10,11], where D^+ is the diffusivity of the ion being charged.

With potential microfluidic applications in mind, Ajdari [12] predicted that asymmetric AC electroosmotic vortices on asymmetric planar electrodes can lead to a net flow instead of the closed circulation within vortices. This AC electroosmotic pump was demonstrated experimentally by Brown [13].

Linear DC electroosmotic flow around particles of the same zeta potential toward an electrode surface with a different polarization can produce vortices when the particles are close to the electrode surface [14,15]. These vortices are on the side of the particles away from the surface. They can hence induce parallel motion of the particles due to hydrodynamic interaction between two adjacent particles. This hydrodynamic interaction is attractive and leads to lateral particle self-assembly.

With AC electroosmosis, the velocities are much larger but the external-field-induced nonuniform polarization produces parallel dipoles on two adjacent particles. Electrostatic interaction between these induced dipoles is attractive for two particles along the same field line. This interaction is responsible for linear self-assembly along field lines [16]. The electrostatic interaction is repulsive for par-

S0021-9797(04)00355-8/FLA AID:10153 Vol.●●●(●●●)
ELSGMLTM(YJCIS):m5 2004/04/06 Prn:9/04/2004; 15:00
yjcis10153
P.4 (1-15)
by:R.M. p. 4

allel self-assembly of particles on different field lines. The electrostatic repulsion between these dipoles then competes with the attractive hydrodynamic forces in the parallel self-assembly dynamics. However, as observed and analyzed by Trau et al. [17], Yeh et al. [18], and Nadal et al. [19], spontaneous self-assembly of colloids on electrode surfaces and even in the bulk [20] occurs with nonlinear AC electroosmosis. Hence, self-assembly seems to occur more readily due to the induced electrostatic dipoles and the hydrodynamic vortices generated by AC nonlinear electrokinetics.

1.3. DC nonlinear and nonequilibrium electrokinetics

All AC electrokinetic phenomena are necessarily nonlinear and nonequilibrium and are hence very prevalent. Nonlinear DC phenomena, on the other hand, is less common.

We have observed and analyzed one such nonlinear DC electrokinetic phenomenon recently [21]. A large field penetration exists near sharp channel corners even for channels made with low-permittivity dielectrics. Hence, the external field can penetrate the double layers on both sides of the corner and also through the corner dielectric in between. This normal field penetration is inward at one side and outward on the other. As such, its field-induced polarization is of opposite charge on the two sides. This produces a converging nonlinear electroosmotic flow that yields an observable microjet and vortex at the corner—both are impossible with linear electrokinetics. Significant particle aggregation occurs at this corner due to this nonuniform channel polarization. Aggregation is absent away from the corner, as is consistent with linear electrokinetics, but occurs at the corner due to the localized nonlinear electrokinetics.

The other and more common DC nonlinear electrokinetic phenomenon is the "electrokinetic phenomenon of the second kind" first envisioned by Dukhin (see review in [22]). It involves a highly conductive and ion-selective granule that permits the external field and diffusion to drive a flux of counterions (a current) into half of a granule. (The co-ions cannot be driven into the other half due to the ion specificity.) This steady flux of ions immediately renders the potential and concentration distributions within the double layer to be different from the Boltzmann equilibrium distributions that cannot sustain a flux. Since this flux is provided by the electromigration of ions driven by the external field, the external field necessarily penetrates the double layer and the latter's polarization is dependent on the normal external field.

Dukhin and Mishchuk have formulated a theory for this DC nonlinear electrokinetic phenomenon (see review [23]). It implicitly assumes that there is a period of transient charging by the external field that builds up a concentrated cloud of counterions at the surface. This charging is intense because the granule is conductive and attracts the external field lines. Although the ion-selective granule is permeable to the counterions, the flux into the granule is much less than the external electromigration flux such that there is a net accumulation of the counterions at the surface. However, this polarization eventually screens the external field to stop the transient charging. Nevertheless, the accumulated counterions, held in place by opposite charges in the granule to maintain a constant potential for the high-conducting granule, do not disperse and effectively produce a nonuniformly charged sphere which screens the external field.

Dukhin argued that knowledge about this residue charge from transient charging is unnecessary to determine the steady-state electrophoretic velocity. His theory yields a rather surprising prediction that the electrophoretic velocity of a spherical granule of radius a scales as

$$U_e \sim O\left(\frac{\hat{\epsilon} E_\infty^2 a}{\mu}\right). \tag{2}$$

In place of the ζ potential, which is typically less than 100 mV, is a potential drop of $E_\infty a$ which can be as large as 10 V for large fields and large particles. A much larger electrophoretic velocity is hence expected. Although the phenomenon is driven by an ion current flux, neither the electrolyte concentration nor the diffusivity appears in the estimate. More elaborate models have been proposed and reviewed in Mishchuk and Dukhin [23] but all have this peculiar scaling.

Many of the features expected of nonlinear electrokinetics have been observed for this DC "electrokinetic phenomenon" of the second kind. Large vortices on the side receiving the counterion flux are predicted by Dukhin [22] and observed by Mishchuk and Takhistov [24]. Also, Barany et al. [25] have reported nonlinear electrophoretic velocities of such particles that are two orders of magnitude higher than linear electrophoresis—a dramatic demonstration of the dominance of nonlinear electrokinetics over linear electrokinetics. However, Dukhin's scaling (2) disagrees with the measurement of Barany et al. beyond a critical applied field. This suggests that the high-field polarization is not due to the transient charging assumed in Dukhin's model. Instead, another physical phenomenon has interfered such that the transient charging in Dukhin's model cannot lead to maximum polarization that completely screens the external field. We shall show that tangential convection is the new phenomenon in play at high fields. As the external field is never completely screened (viz., the particle is electrically insulated from the outside) due to this new mechanism, a steady current persists into the granule at steady state.

In this paper, we shall examine the various conditions required for DC nonlinear electrokinetics in general. In particular, we shall mathematically specify the implicit assumptions leading to (2) and examine why Dukhin's phenomenon requires a conducting and ion-specific granule. In the process, a theory will be offered for when complete screening occurs and why scaling (2) breaks down beyond a critical applied field.

2. Formulation

Although charging of the polarized layer can be either transient or steady, we shall focus only on the final steady state for a spherical granule. If the steady state corresponds to complete external field screening, the charging must be transient. The dimensionless governing equations for a spherical coordinate whose origin lies at the sphere center are the standard Poisson equation for electrostatics, the steady ion-flux transport equations that include convective flux and the viscous flow equations driven by the Maxwell stress on regions with a net charge:

$$\epsilon^2\nabla^2\phi = C^- - C^+, \tag{3}$$

$$P\mathbf{u}\cdot\nabla C^{\pm} = -\nabla\cdot\mathbf{J}^{\pm}, \tag{4}$$

$$\mathbf{J}^{\pm} = -K^{\pm}(\pm C^{\pm}\nabla\phi + \nabla C^{\pm}), \tag{5}$$

$$\nabla^2\mathbf{u} - \nabla p = -\nabla^2\phi\nabla\phi, \tag{6}$$

where $\mathbf{u}$ is the fluid velocity, $\mathbf{J}^{\pm}$ is the combined diffusive and electromigration fluxes of the cation and anion in vectorial form, $K^{\pm} = D^{\pm}/D$, $D^{\pm}$ are the cation and co-ion diffusivities and $D = (2D^+D^-)/(D^+ + D^-)$. Both $K^{\pm}$ and D are assumed to be unit order parameters—the diffusivity ratio is not excessive for the cations and anions. They are of $O(\epsilon^0)$ relative to the expansion parameter ϵ. The inhomogeneous term in (6) represents the Maxwell stress $(C^+ - C^-)\nabla\phi$ due to polarization $C^+ \neq C^-$. For simplicity, we have assumed a 1:1 electrolyte with single-valent anions and cations.

In scaling Eqs. (3)–(6) we have used as the characteristic concentration the bulk value C_∞, the characteristic potential $RT/F = 25.7$ mV, the characteristic pressure $P_0 = \mu U_0/a$ and the characteristic length a (granule radius). The characteristic velocity is $U_0 = (\hat{\epsilon}/\mu a)(RT/F)^2$ which is the linear Smoluchowski slip velocity of a surface with a zeta potential ζ of RT/F and a reference applied field of $E_0 = RT/Fa$. The parameter $\hat{\epsilon}$ is the electrolyte permittivity (the dielectric constant). The reference Peclet number is $P = U_0 a/D$ with this scaling. However, the true Peclet number should be $Pe = U_e a/D^+$, where U_e is the yet unknown electrophoretic velocity. It should be much larger than P and will be estimated subsequently.

Equations (3)–(6) will be solved with surface and far-field boundary conditions. The far-field conditions are obvious—a unidirectional applied field $-E_\infty\hat{e}_z$, an electroneutral and homogeneous Ohmic bulk $C^- = C^+ = 1$ and, in the absence of any external pressure driven flow, a vanishing velocity field if the solid is stationary.

The surface condition for the velocity field is the usual no-slip condition. We shall examine both a specified surface field E_s and an isopotential surface for surfaces with large permittivity or high conductivity. With field penetration, the granule surface and the bulk electrolyte are no longer electrically insulated and decoupled. As such, the exact potential value for the isopotential granule must be selected carefully for nonequilibrium conditions.

For equilibrium ion distributions that do not sustain a net flux, the surface concentration is specified by the potential difference with the bulk via the Boltzmann distribution. There is hence no need for a surface condition for ions that have equilibrated. When there is a net flux into the surface, we specify the surface concentration C_s^+ by assuming that the ion concentration near the surface is determined by an adsorption isotherm. The counterion must first adsorb onto the surface before it enters the solid. In the expected limit when the adsorption kinetics are fast compared to the slow transport rate, an adsorption equilibrium is established. The equilibrium surface concentration is determined by kinetic equilibrium of the surface chemistry and not by the Boltzmann equilibrium distributions. The former equilibrium is at the surface and it permits an ion flux in the polarized region. The latter equilibrium is over the entire polarized region and allows no net flux.

Specifying both C_s^+ and a constant surface potential seems contradictory, as the surface counterions would introduce a field into the solid. However, for a solid with a sufficiently large permittivity or conductivity, this field does not produce a significant potential gradient in the solid. For high-permittivity particles, this limit occurs when $\hat{\epsilon_p}/\hat{\epsilon} \gg 1$, where $\hat{\epsilon_p}$ is particle permittivity. A similar condition applies for conductivity. For a very conducting solid, opposite charges in the solid would migrate rapidly to the surface to offset the counterions on the other side. If the opposite charges are not mobile in the solid, like charges would move away from the surface to produce a surface region of opposite charge on the solid side. This "double layer" ensures a constant-potential surface.

However, the small parameter ϵ will introduce two or three regions with two length scales. The boundary conditions for each region are obtained via matched asymptotics with adjacent regions. Hence, the external velocity and potential fields will not see the true surface conditions but certain effective ones. These effective conditions will be the objective of our derivation. We will specify the true and effective conditions subsequently when each region is analyzed.

The small parameter

$$\epsilon = \lambda/a \tag{7}$$

is the ratio of the Debye thickness to the granule radius. We seek an expansion about ϵ. Although there is no surface field E_s to screen in this nonequilibrium case, the penetrating external field will be screened by the ions that electromigration and diffusion have driven to the surface. The external field is screened by a thin near-equilibrium layer near the surface but also by an extended polarized region beyond it. Nevertheless, the screening length of any electric field is λ, which is the screening length for the surface field in equilibrium Debye layers. We hence expect the thickness of the entire polarized region, which screens the external field, to be λ.

Except for a thin polarized inner region near the surface, whose thickness is of order ϵ, we can set ϵ to zero in the

S0021-9797(04)00355-8/FLA AID:10153 Vol.●●●(●●●)
ELSGMLTM(YJCIS):m5 2004/04/06 Prn:9/04/2004; 15:00
yjcis10153
P.6(1-15)
by:R.M. p. 6

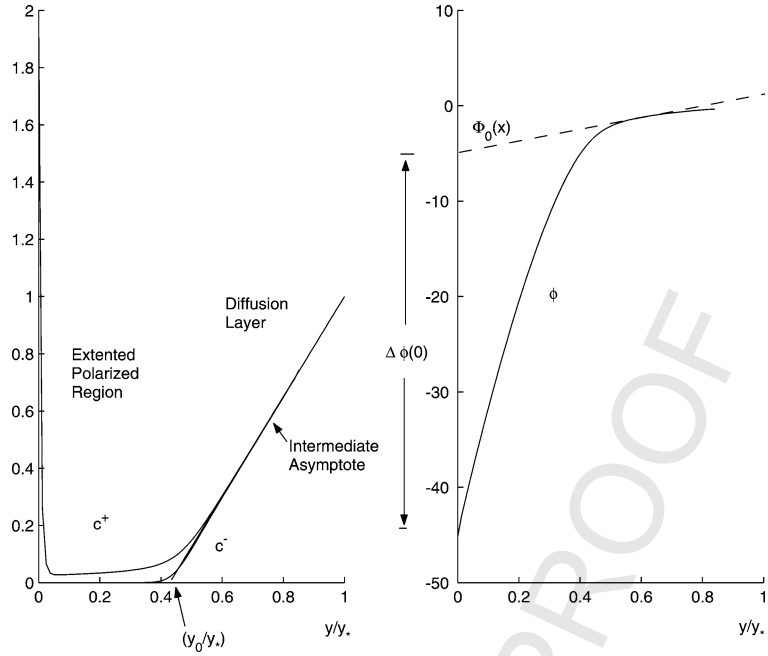

Fig. 2. Numerical solution of the nonequilibrium polarized region for $C_s^+ = 2$, $\epsilon = 0.01$ and $j^+/K^+ = 3.5$. The potential drop $\Delta\phi(0)$ is nonuniform and dependent on external field Φ.

electrostatic equation (3). This implies that electroneutrality $C^+ = C^-$ exists everywhere except within the thin polarized inner region. Electroneutrality, however, does not guarantee a homogeneous concentration distribution. Far from the granule, the concentration is indeed uniform at the bulk value for the outer Ohmic region. However, an electroneutral intermediate diffusion layer region with concentration gradient exists between the inner and outer regions (compare Fig. 2 to Fig. 1). In both outer and intermediate electroneutral regions, one with a nonuniform concentration field and one with a uniform field, the electrostatic problem reduces to the Laplace equation

$$\nabla^2\Phi = 0 \tag{8}$$

and satisfies the far-field condition imposed by a unidirectional applied field $E_\infty = -\nabla\Phi(r\to\infty) = -E_\infty\hat{e}_z$ in the axial axis of the cylindrical coordinate. The external potential within both electroneutral regions will be denoted Φ.

The inner potential ϕ within the polarized layer of thickness ϵ must match the external potential Φ described by the Laplace equation (8) (see Fig. 2):

$$\phi(y\to\infty) = \Phi(r=0) = \Phi_0, \tag{9}$$

$$\frac{\partial\phi}{\partial y}(y\to\infty) = \frac{\partial\Phi}{\partial r}(r=0) = \left(\frac{\partial\Phi}{\partial r}\right)_0. \tag{10}$$

We have assumed a spherical granule. More importantly, with the present scaling $y \sim O(1)$ at the granule length scale and the limit of $y\to\infty$ is strictly incorrect and should be $y/\epsilon\to\infty$. We shall omit the tedious inner scaling $y\to y/\epsilon$ unless it is absolutely required in the analysis. The formally correct representation should be obvious in context.

A most important feature of this ion-flux-induced polarization is the existence of a diffusion layer. In an equilibrium Debye layer, the counterion concentration decreases outward to allow diffusion flux out to balance electromigration flux in (see Fig. 1). Hence, to produce a net flux in, we expect the concentration gradient to change sign such that diffusion and electromigration complement each other. This positive concentration gradient should exist near the electroneutral edge of the polarized layer where the field and electromigration are weakest. Consequently, the co-ion concentration also increases outward with the same slope. We hence expect an electroneutral region with spatially inhomogeneous (increasing outward) concentration to sandwich between the polarized region and the Ohmic region with electroneutral and homogeneous concentrations.

We have numerically constructed some typical constant-flux steady-state concentration profiles near the surface that sustain an ion flux [26]. A reproduction of the computed profiles in Fig. 2 shows the electroneutral intermediate asymptote with a positive gradient. This asymptote connects the polarized region with the electroneutral diffusion layer. The diffusion layer, in turn, lies between the polarized layer and the Ohmic bulk. The diffusion layer resembles classical diffusion layers dominated by diffusion or diffusion and tangential convection, except normal electromigration also plays a role. In our earlier theory [26], tangential connection was not explicitly included. This will be remedied here with a two-dimensional matched asymptotic analysis for large Peclet numbers.

An important consequence of the positive concentration gradient between the diffusion layer and the polarized layer is the presence of an extended polarized region with excess

S0021-9797(04)00355-8/FLA AID:10153 Vol.●●●(●●●)
ELSGMLTM(YJCIS):m5 2004/04/06 Prn:9/04/2004; 15:00
yjcis10153
P.7(1-15)
by:R.M. p. 7

space charge (compare Fig. 2 to Fig. 1). This region extends the polarization from the Debye layer into the diffusion layer. In subsequent sections, we shall carry out matched asymptotics from the polarized layer, across the diffusion layer and into the Ohmic region. The objective is to obtain an effective steady-state boundary condition for the Laplace equation (8) that reflects the steady-state screening by the extended polarized region. However, we shall precede this with a general discussion on the necessary conditions for nonlinear electrokinetics.

3. Polarized region

3.1. Maxwell stress and liquid motion

We first focus on the long-wave expansion of the equations of motion (6) for $\epsilon \ll 1$ within the thin polarized region. The normal momentum balance is entirely hydrostatic and we obtain a Maxwell pressure

$$p \sim P_0(x) + \frac{1}{2}\left[\left(\frac{\partial\phi}{\partial y}\right)^2 - \left(\frac{\partial\Phi}{\partial r}\right)_0^2\right],$$

where $P_0(x)$ is the bulk pressure on the surface. We shall assume that a bulk pressure gradient does not exist (pure electrokinetics) and set the homogeneous P_0 to an arbitrary constant. Substituting the Maxwell pressure into the tangential momentum balance, we obtain for $\partial/\partial y \gg \partial/\partial x$

$$\frac{\partial^2 u}{\partial y^2} = \frac{1}{2}\frac{\partial}{\partial x}\left[\left(\frac{\partial\phi}{\partial y}\right)^2 - \left(\frac{\partial\Phi}{\partial r}\right)_0^2\right] - \frac{\partial^2\phi}{\partial y^2}\frac{\partial\phi}{\partial x}. \tag{11}$$

This equation must be solved with the no-slip boundary conditions $u(y=0)=0$ and the far-field condition $(\partial u/\partial y)(y\to\infty)=0$. The latter because we expect the velocity to approach a constant asymptote when it exits the polarized layer and the Maxwell force disappears. It is the constant asymptote that defines the slip velocity U_s for the electroneutral diffusion layer region and the Ohmic region.

We would like to convert the Maxwell stress on the right of (11) in such a manner that the asymptotic slip $U_s = \lim_{y\to\infty} u(y)$ is a product of the tangential external field $-\partial\Phi/\partial\theta$ and the potential drop across the polarized layer $\phi(0)-\Phi_0$. This is the manner the classical slip Smoluchowski velocity (1) is expressed and is intuitively correct. The difference for nonlinear electrokinetics is simply that the potential drop $\phi(0)-\Phi_0$ is a function of $(\partial\Phi/\partial r)_0$.

There are two specific scalings that render this from possible. In the stretched coordinates of the polarized region, they are

$$\phi(x,y) = \Delta\phi(\epsilon x, y) + \lim_{r\to 1}\epsilon^{1/2}\Phi\big(\epsilon(r-1),\theta\big) \sim \Delta\phi(y) + \epsilon^{1/2}\Phi_0(\theta), \tag{12}$$

$$\phi(x,y) = \Delta\phi(\epsilon x, y) + \lim_{r\to 1}\epsilon^{1/2}\Phi(r,\theta) \sim \Delta\phi(y) + \epsilon^{1/2}\Phi_0(\theta), \tag{13}$$

where $\Delta\phi(y)$ is the potential drop relative to the external potential $\epsilon^{1/2}\Phi$, which is assumed to be smaller due to the high field and large potential drop within the polarized layer (see Fig. 2).

Due to the condition $(\lambda/a)\ll 1$, the potential drop $\Delta\phi$ is only weakly dependent on x for both cases. However, condition (12) reflects a nearly screened external field such that $(\partial\Phi/\partial r)_0 \sim O(\epsilon)$ is nearly zero and the particle is nearly insulated electrically from the bulk electrolyte. Scaling (13), however, allows an external field that is oblique to the granule, $(\partial\Phi/\partial r)_0 \sim O(1)$. We exclude the case of weak screening, $(\partial\Phi/\partial r)_0 \sim O(\epsilon^{-1}) \gg 1$. In this unscreened limit, which occurs before the polarization builds up, the tangential variation of the inner potential ϕ is as strong as that of the external potential Φ. As such, the first normal stress term in (11) cannot be omitted and the Maxwell stress is not integrable. At steady state, when the surface is fully polarized by the charging current, strong external field screening with $(\partial\Phi/\partial r)_0$ of unit order and smaller is the appropriate boundary condition.

We note that the screening of external field in (12) is not due to the counterions attracted by the surface charge, as is the case for equilibrium linear electrokinetics. Rather, it is by the ions driven by the external field and by diffusion. The charging occurs over a short transient before it reaches a steady state with a constant flux that may be vanishingly small. If the steady state corresponds to complete screening of external field, the transient charging time has been estimated to be $\lambda a/D^+$ by Squires and Bazant [11]. If the steady state corresponds to one with partial external field penetration, the charging time is even shorter. In the former case, the charges within the polarized layer are accumulated during the charging transient. In the latter case, the charges after the transient are supplied by electromigration from the bulk. In both cases, every charge in the polarized layer is compensated by an opposite charge in a conducting granule with an isopotential surface (see Fig. 3). However, the polarization, whether due to transient or steady charging, is not limited by the surface charge and the capacitance of the polarized layer is determined only by the external field.

With both scalings, (11) becomes to leading order in ϵ in the unstretched coordinates

$$\frac{\partial^2 u}{\partial y^2} = -\frac{\partial^2}{\partial y^2}\Delta\phi\left(\frac{\partial\Phi}{\partial\theta}\right)_0. \tag{14}$$

The hydrostatic pressure gradient does not contribute as the Maxwell normal stress is independent of the tangential coordinate with these scalings.

Integrating (14) with the no-slip and far-field boundary conditions and realizing from the matching conditions (9) and (10) that $\Delta\phi(y\to\infty) = (\partial\Delta\phi/\partial y)(y\to\infty) = 0$, we obtain the desired form

$$U_s = \Delta\phi(0)\left(\frac{\partial\Phi}{\partial\theta}\right)_0 = \big(\phi(0)-\Phi_0\big)\left(\frac{\partial\Phi}{\partial\theta}\right)_0. \tag{15}$$

S0021-9797(04)00355-8/FLA AID:10153 Vol.●●●(●●●)
ELSGMLTM(YJCIS):m5 2004/04/06 Prn:9/04/2004; 15:00
yjcis10153
P.8(1-15)
by:R.M. p. 8

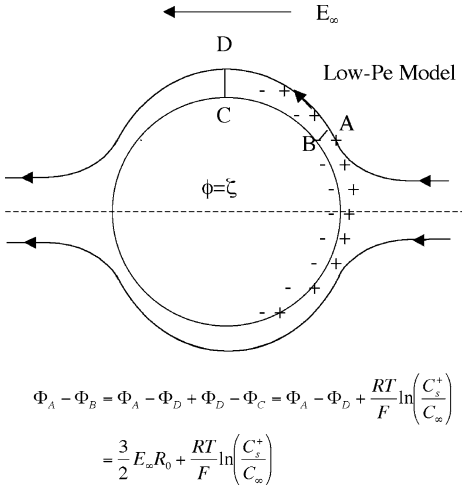

Fig. 3. Our low-*Pe* model with significant screening of the Ohmic field. The granule potential is constant and the potential drop across CD is fixed by an equilibrium zeta potential ζ. The charges in the polarized layer are counterbalanced by opposite internal charges to maintain a constant-potential surface.

For a surface with a large electric field E_s imposed by the surface charges, the Debye layer is at equilibrium and the potential drop across the Debye layer $\Delta\phi(0)$ in (15) is independent of position and the outer potential Φ_0 (see Fig. 1). For a conducting granule, however, the surface potential $\phi(0)$ is constant. Consequently, the potential drop $\Delta\phi(0) = \phi(0) - \Phi_0$ is dependent on Φ_0. In fact, for the latter case, we can integrate (15) explicitly to obtain an estimate of the average slip velocity $\langle u_s\rangle_{1/2}$ over the front hemisphere of the sphere in Fig. 3,

$$\langle u_s\rangle_{1/2} = \left[\phi(0)\Delta\Phi_0 - \frac{1}{2}(\Delta\Phi)^2\right]\Big/(\pi/2), \tag{16}$$

where $\Delta\Phi_0$ is the Ohmic potential drop from the pole to the equator on the surface of the sphere. Because polarization occurs only over the front hemisphere, we shall show the average slip velocity over this surface $\langle u_s\rangle_{1/2}$ provides a good estimate of the electrophoretic velocity. The granule potential $\phi(0)$ remains to be specified.

The external potential drop $\Delta\Phi(0)$ around the granule is of $O(E_\infty a)$ for the scalings of (12) and (13). Hence, in the limit of large E_∞, the second term in (16) dominates. Moreover, the magnitude of this term is determined by the degree of external field screening. The slip velocity reaches a maximum when there is complete exclusion of the external field due to the polarization created during transient charging. This explains why the Dukhin scaling (2) is independent of ion diffusivity and ion concentration. This observation will be quantified more explicitly in our analysis.

3.2. Poisson equation and surface conditions

For both steady and transient charging, the potential drop $\Delta\phi(0)$ must be determined from the expanded Poisson equation in the polarized layer:

$$\epsilon^2\frac{\partial^2}{\partial y^2}\Delta\phi = C^- - C^+. \tag{17}$$

For a surface with specified surface field, (17) must be solved with

$$\frac{\partial\Delta\phi}{\partial y}(0) = -E_s. \tag{18}$$

Without external field penetration, this surface field induces an equilibrium Debye $\Delta\phi_{\rm eq}$ potential that obeys

$$\epsilon^2\frac{\partial^2}{\partial y^2}\Delta\phi_{\rm eq} = e^{\Delta\phi_{\rm eq}} - e^{-\Delta\phi_{\rm eq}}, \tag{19}$$

where the Boltzmann equilibrium distributions have been inserted.

By perturbing from the equilibrium concentration, we can demonstrate small external field leakage is not possible with a specified surface field (18). The perturbation field be $\phi' = \Delta\phi - \Delta\phi_{\rm eq}$ obeys the linearized Poisson equation

$$\epsilon^2\frac{\partial^2}{\partial y^2}\phi' = (e^{\Delta\phi_{\rm eq}} + e^{\Delta\phi_{\rm eq}})\phi'. \tag{20}$$

Comparing this to (19), we conclude that $\phi' = (d/dy)\Delta\phi_{\rm eq}$. However, since the surface filed is fixed in (18), the appropriate boundary condition for ϕ' is $(d\phi'/dy)(0) = 0$.

This zero excess surface field penetration cannot be satisfied by $(d^2/dy^2)\Delta\phi_{\rm eq}(0) = \epsilon^{-2}[C^-(0) - C^+(0)] \neq 0$. Moreover, $(d/dy)\Delta\phi_{\rm eq}$ blows up exponentially and cannot allow matching with Φ as stipulated in (9) and (10). We are hence unable to perturb the equilibrium Debye layer with boundary condition (17) for $(\lambda/a) \ll 1$. Nonequilibrium and nonlinear electrokinetics cannot occur for thin Debye layers if the surface field is fixed. Mathematically, it implies that the linearized operator is not invertible—the solvability condition cannot be satisfied. The singularity of this operator is related to the fact that the equilibrium potential distribution $\phi_{\rm eq} = \Phi_0 + \Delta\phi_{\rm eq}$ is invariant to a constant shift (a change in the reference point). The pertinent variable with a specified surface field is not the potential but the potential drop relative to the bulk value.

This then explains the choice of a conducting granule by Dukhin. It is insufficient that the granule permits flux of counterions. It must also permit field penetration into the surface during transient or steady changing to allow a departure from equilibrium in the polarized region. This surface field penetration implies that there cannot be bound surface charges which generates a large fixed surface field $E_s \sim O(\epsilon^0)$. For a constant-potential conducting granule, the constant granule potential $\phi(0)$ offers a specific reference point and the potential ϕ in the polarized layer cannot be arbitrarily shifted. Perturbation from equilibrium is now possible.

The reference granule potential $\phi(0)$ remains to be specified for the steady-state problem. In fact, Dukhin neglects it in comparison to the external potential on the surface Φ_0.

This argument requires some scrutiny. The concentration depletion due to the diffusion layer, as seen in Fig. 2, significantly reduces the conductivity in the electroneutral region. As such, there is a significant potential drop across both the diffusion and polarized layers. However, this polarization disappears at the equatorial position (point D in Fig. 3) since the normal external field, $(\partial\Phi/\partial\theta)$, is exactly zero and screening is absent.

The surface concentration $C_s^+ > 1$ is established by adsorption equilibrium. Since there is no field penetration and flux at the equator D, it also sustains an equilibrium Debye layer. The potential drop across this equational Debye layer, the difference between the constant granule potential and the external potential, at the equator is related to C_s through the Boltzmann equilibrium relationship. At the equator, C_s^+ is hence consistent with both an adsorption equilibrium and a Boltzmann equilibrium in the electrolyte due to the potential drop across the polarized layer. Hence, a zeta potential ζ exists due to the adsorption isotherm rather than surface field by bound charges,

$$\Phi_D - \phi_C = \frac{RT}{F}\ln C_s^+ \equiv \zeta. \tag{21}$$

Since the granule is at the same potential, the constant granule potential in (15) is now specified

$$\phi(0) = \Phi_D - \zeta. \tag{22}$$

We can arbitrarily assign $\Phi_D = 0$ to be the reference point of the entire potential field.

We note that the slip velocity expression (15), with a potential drop $\Delta\phi(0)$ across the polarized layer, also applied for linear electrokinetics with surface-field-induced polarization. In that case, however, the external field is not present in the Debye layer (see Fig. 1). As such, $\Delta\phi(0)$ is independent of the surface value of the external potential Φ_0 and the tangential coordinate x. Hence, choosing the external reference potential to be zero, $\Delta\phi(0) = \phi(0) = -\zeta$ for linear electrokinetics.

3.3. Dukhin's maximum electrokinetic velocity

With the specification of the potential reference point $\Phi_D = 0$ and $\phi(0) = -\zeta$, we are in the position to evaluate Dukhin's slip velocity at steady state. We examine his limit, when all the polarization is done during transient charging. The charging stops when the external field is completely screened. However, the polarization remains in place due to the attraction between the charges within the polarized layer and the opposite charges they have attracted on the granule side (see Fig. 3). Both have arrived at their positions during the transient charging. Due to (15), the exact charge within the polarized region, for this maximum charging limit, does not need to be known.

With this leading-order insulated condition $(\partial\Phi/\partial r)(r = 1) = 0$ for the Laplace equation (8) of the external potential, we obtain

$$\Phi(r,\theta) = E_\infty z\left(1 + \frac{1}{2r^3}\right), \tag{23}$$

where $\Phi(1,\pi/2) = \Phi_0(\pi/2) = 0$ because of the designated reference point.

The local slip velocity is then, from (16),

$$U_s = \frac{3}{2}\zeta E_\infty + \frac{9}{8}\sin 2\theta E_\infty^2. \tag{24}$$

Although there is a large hydrodynamic stress of $O(\mu U_e/\lambda)$ in the flow field (6) within the inner polarized layer, this thin film does not entrain or eject fluid appreciably from the surrounding fluid for a moving granule undergoing electrophoresis or for a stationary granule driving an electroosmostic flow around it. Hence, the film within the polarized layer can be assumed to move with the particle in electrophoresis. Consequently, in both electrophoresis and electroosmosis, the viscous drag on both granule and film should be obtained from the effective Ohmic velocity U_s of (16) and not the inner velocity $u = 0$. The electroosmotic viscous drag exerted by the slip velocity (16) can be easily evaluated from a harmonic expansion of the axisymmetric spherical biharmonic expansion from $\nabla^2\mathbf{u} = \nabla p$. It is

$$D = 3\pi\left(2\zeta E_\infty + \frac{9}{4}E_\infty^2\right). \tag{25}$$

Only the front half of the granule is involved in (25) as the counterions only enter in this half. There is insignificant drag in the back half as only the uniform linear Smoluchowski electroosmotic velocity ζE_∞ exists there. In fact, due to co-ions accumulation in the back half, we expect the tangential field to be weak there and the slip velocity to be even smaller than the Smoluchowski slip.

The drag in (25) corresponds to the drag on a stationary granule by the electroosmotic flow around it. To evaluate the electrophoretic drag, we shift to a frame moving with the electrophoretic velocity U_e. This corresponds to a shift of the electroosmotic velocity field by a uniform velocity field $U_e\hat{e_z}$. Since this uniform reference velocity is stress-free, the electrophoretic drag is same as the electroosmotic drag D. However, the surface tangential velocity $U_s(\theta) - U_e\cos\theta$ should be nearly zero in the moving frame, since it is the slip velocity that drives the motion. Hence, we can shrink the granule into a point and use the Stokes drag $6\pi U_e$ for a point particle without slip. This produces an estimate for the electrophoresis velocity

$$|U_e| = \zeta E_\infty + \frac{9}{8}E_\infty^2, \tag{26}$$

or in dimensional form

$$|U_e| = \frac{\hat{\epsilon}\zeta E_\infty}{\mu} + \frac{9}{8}\frac{\hat{\epsilon}}{\mu}E_\infty^2 a. \tag{27}$$

Because of the integrable form of the Maxwell stress in (14) due to scaling (12), in the limit of maximum screening, we have found it unnecessary to resolve the polarized

S0021-9797(04)00355-8/FLA AID:10153 Vol.●●●(●●●)
ELSGMLTM(YJCIS):m5 2004/04/06 Prn:9/04/2004; 15:00
yjcis10153
P.10 (1-15)
by:R.M. p. 10

layer in deriving (24) and (26). However, to determine when this maximum velocity limit is valid (whether complete screening can be reached) and to correct it when it is not (when there is significant external field leakage at steady state), we shall need to carry out the matched asymptotics required to resolve the steady-state polarized region and diffusion layer. This analysis will be preceded by the derivation of an important asymptote of the polarized region.

3.4. Electroneutral asymptote of polarized layer

In the limit of small ϵ, the ion transport equations in the polarized layer are

$$\epsilon^2 \frac{\partial^2 \phi}{\partial y^2} = C^- - C^+, \tag{28}$$

$$C^+ \frac{\partial \phi}{\partial y} + \frac{\partial C^+}{\partial y} = -j^+/K^+, \tag{29}$$

$$-C^- \frac{\partial \phi}{\partial y} + \frac{\partial C^-}{\partial y} = 0, \tag{30}$$

which must be solved with surface boundary conditions

$$\phi(y=0) = \zeta, \tag{31}$$

$$C^+(y=0) = C_s^+. \tag{32}$$

Note that the counterion flux j^+ is negative.

It is still an unknown quantity that must be determined by matched asymptotics with the diffusion layer that specifies the flux. In fact, its relationship with Φ_0 provides the desired condition for the outer equation (8).

As complex as (28)–(30) seem, its asymptotic behavior at large y can be derived explicitly by invoking the electroneutral limit $C^- = C^+ = \bar{C}$ [26]. This asymptote is

$$\frac{\partial \bar{C}}{\partial y} = -\frac{j^+}{2K^+}. \tag{33}$$

Alternatively, one can designate the position y_* as the nominal position where the asymptotic concentration $\bar{C}$ reaches unity (see Fig. 2):

$$\bar{C} = 1 - \frac{j^+}{2K^+}(y - y_*). \tag{34}$$

This electroneutral asymptotic behavior of the polarized region is independent of the *Pe* number for the diffusion layer. The unit bulk concentration is only reached beyond the diffusion layer and into the Ohmic region (see Fig. 2). Nevertheless, y_* is a nominal asymptotic position that estimates the thickness of the diffusion layer. Its value must be estimated via matched asymptotics and this value is dependent on the *Pe* number in the diffusion layer.

In [26], we have matched the solution of (28)–(30) with surface boundary conditions (31) and (32) to the asymptotic limit (34). The analysis is simplified by several symmetries of the equation. The zeta potential ζ can be eliminated by a simple shift of ϕ. The parameters ϵ and j^+/K^+ can be transformed away with the transformation $\eta = \exp(\phi/2)/(\epsilon j^+/K^+)^{1/3}$ and $\xi = (j^+/K^+)^{1/3} y/\epsilon^{2/3}$. Only a scaled surface concentration C_s^+ remains at the boundary condition and all three equations collapse into a single second Painléve equation without parameters. An asymptotic analysis of the limiting Airy equation at large j^+ shows the result to be insensitive to C_s^+ and ζ.

In this limit of large j^+, we hence obtain a universal correlation insensitive to ζ and C_s^+. The asymptotic potential at y_* is shown to be

$$\phi(y_*) = -\frac{j^+}{K^+}\frac{y_*^2}{3\epsilon} - \frac{2}{3}\left(\frac{y_*}{\epsilon}\right).$$

Using the matching conditions (9) and (10) and realizing that $j^+/K^+ = (\partial\phi/\partial y)(y \to \infty) = (\partial\Phi/\partial r)_0$, this can be written as

$$\beta\left(\frac{\partial \Phi}{\partial r}\right)_0 = \Phi_0 + V, \tag{35}$$

where the screening length $\beta = (y_*^2/3\epsilon)$ and $V = \frac{2}{3}(y_*/\epsilon)$ are two constant coefficients.

Boundary condition (35) represents an effective boundary condition for the Laplace equation (8) of the external potential Φ. For scalings (12) and (13) to be valid, the effective screening length β must a unit-order number or larger with respect to ϵ. If the screening length β exceeds the granule radius, the steady-state external field penetration is insignificant. If it is of the order of the granule radius, however, significant penetration occurs. It remains to determine y_* from matched asymptotics with the diffusion layer of both small and large *Pe*. However, in the limit of $(3\epsilon/y_*^2) \ll 1$, when there is maximum polarization and minimum field penetration, the maximum Dukhin slip velocity (15) can be derived without explicit construction of the potential and concentration profiles by matched asymptotics.

4. Low-Peclet theory

For typical zeta potentials (<100 mV) for usual electrolyte concentrations, the electrophoretic mobility U_e/E_∞ is typically less than 10^{-4} cm^2/V s. Hence, if E_∞ is roughly or smaller than $(RT/F)/a$, the Peclet number $Pe = U_e a/D$ is less than unity for most electrolytes. Larger mobilities are expected with nonlinear electrokinetics. However, we still expect $Pe \sim 0(\epsilon)$ to be small. We shall show that this low-*Pe* limit produces a completely screened steady state.

With low *Pe*, the tangential convection term can be neglected from the transport equation (4) and one obtains

$$\frac{1}{r^2}\frac{\partial}{\partial r}\left(r^2 C \frac{\partial \Phi}{\partial r} + r^2 \frac{\partial C}{\partial r}\right) = 0, \tag{36}$$

$$\frac{1}{r^2}\frac{\partial}{\partial r}\left(-r^2 C \frac{\partial \Phi}{\partial r} + r^2 \frac{\partial C}{\partial r}\right) = 0 \tag{37}$$

for the electroneutral concentration in the diffusion layer.

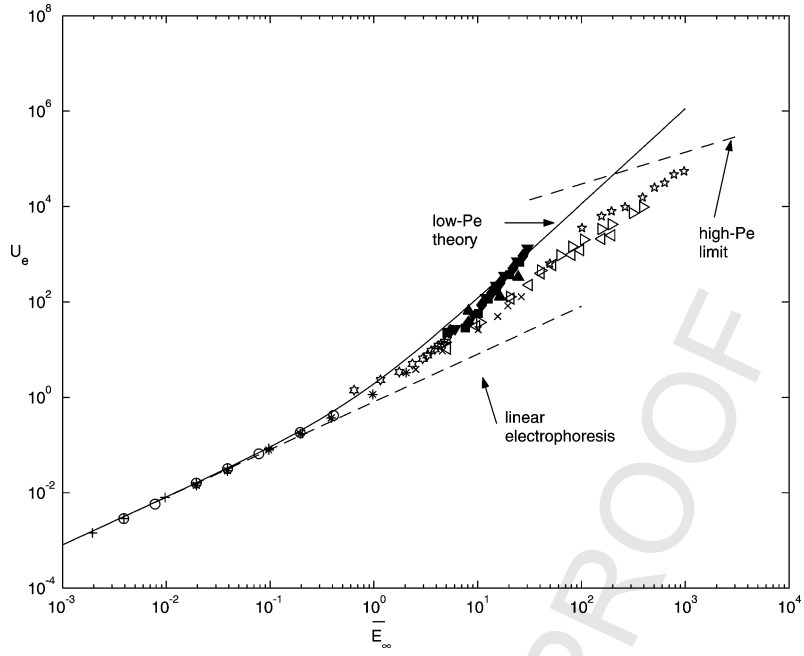

Fig. 4. Three sets of data plotted in the two universal dimensionless parameters of the low-*Pe* theory—$\bar{E}_\infty = E_\infty a/(RT/F)$ and the electrophoretic velocity scaled by the reference velocity $U_0 = (\hat{\epsilon}/\mu a)(RT/F)^2$ with $\hat{\epsilon}$ taken to be 6.9×10^{-10} C^2 N^{-1} m^{-2}. The scaled surface concentration C_s^+/C_∞ is taken to be 5 but the collapse is insensitive to this parameter as it appears only in $\zeta = \ln(C_+^s/C_\infty)$. The particle diameter $2a$ in μm is 0.5 (+), 1 (○), 5 (∗), 25 (×), 260 (■), 280 (◆), 310 (▼), 420 (▲), 50 (◁), 100 (▷), 200 (☆), 27 (✡). The open symbols are Barany et al.'s data, the closed symbols are Mishchuk and Takhistov's data and the six-pointed stars are our experimental data. The solid curve is the low-*Pe* theory (26) and the two dashed straight lines are, respectively, the linear electrophoretic velocity at low field and the large-*Pe* theory $U_e \sim 1.4 \times 10^3 \bar{E}_\infty^{2/3}$ for $a = 175$ μm.

Adding these two equations to remove the electromigration term, we obtain

$$\frac{1}{r^2}\frac{\partial}{\partial r}\left(r^2\frac{\partial C}{\partial r}\right) = 0. \tag{38}$$

The solution of this diffusion equation must match with the Ohmic concentration $C = 1$ at $r \to \infty$. Hence, its solution is

$$C = 1 - \frac{1}{r}\left(\frac{\partial C}{\partial r}\right)(r = 1). \tag{39}$$

Matching the slope of this diffusion layer solution with the slope of the intermediate asymptote (33) of the polarized region, we obtain

$$C(r) = 1 + \frac{j^+}{2K^+}\frac{1}{r}, \tag{40}$$

and the asymptotic concentration on the surface is

$$C(1) = 1 + \frac{j^+}{2K^+} < 1. \tag{41}$$

Similarly, the intermediate asymptote (34) becomes

$$\bar{C} = 1 + \frac{j^+}{2K^+}(1 - y). \tag{42}$$

The position y_* of (34) is specified

$$y_* = 1, \tag{43}$$

and the screening length $\beta = 1/3\epsilon$ is indeed much larger than the unit granule radius, corresponding to the screened case of (12). The quantity y_* is the thickness of the low-*Pe* diffusion layer—the particle radius and the dimensional screening length is the granule radius divided by 3ϵ. One can hence use the insulated condition $(\partial\Phi/\partial r)(r = 1) = 0$ and the Dukhin slip velocity (26) to describe low-*Pe* nonlinear electrophoresis, which is the maximum possible.

While the insulated condition does not allow field penetration and electromigration inward, this is only the leading-order approximation for the external field. The polarized region still sees a flux j^+ provided by high-order effects. The extended polarization region of space charge in Fig. 2 still exists and is, in fact, very thick. Its charges are driven there during transient charging and held in place at steady state by the opposite charges on the granule side and by the steady flux J^+ that represents insignificant leakage to the external field. Equation (16) implies that, for this leading-order insulated case, we do not need to resolve the thick polarized layer.

In Fig. 4, we successfully collapse our recently measured low-field data and those by Barany et al. [25] and Mishchuk and Takhistov [24] by this correlation. (The data of Barany et al. are represented by open symbols and those by Mishchuk closed symbols. Our data are the intermediate ones indicated by six-point stars.) A reasonable value of 5 is used for C_s^+ but this value, the granule counterion concentration scaled by the bulk value, can change by one order of magnitude and still would not affect the theoretical curve significantly. This value of the dimensionless C_s^+ correspond to a dimensional zeta potential of $\zeta = 41$ mV. The granule diameter

$2a$ ranges from 1 to 500 μm and the electric fields range from 1 to 10^3 V/cm and the electrophoretic velocity from 10^{-4} to 10^{-1} cm/s in the data. The electrolyte concentration C_∞ varies from 10^{-5} to 10^{-3} M for various electrolytes ranging from HCl to K_2SO_4. The granule surface ion concentrations C_s^+ must also vary over a large range but their values are not known and are difficult to measure. Yet all data collapse within a factor of two by (26) over 6 decades of dimensionless electric field. As expected, this low-*Pe* result is valid up to a dimensionless E_∞ of unit order (when the applied field is roughly (RT/Fa)). The low-*Pe* theory begins to fail beyond $E_\infty^c \sim 10$, although some data are still described by the theory up to $E_\infty = 30$. The transition from linear to nonlinear electrophoresis occurs at a critical dimensionless external field of $E_\infty \sim 1.0$. This low-*Pe* nonlinear electrophoresis can be 10 to 100 times larger than linear electrophoresis. Beyond $E_\infty = 30$, the Peclet number begins to exceed unity even for the smaller granules and the low-*Pe* theory begins to overestimate the speed. Beyond this critical field, a new physical mechanism stops the transient charging before complete external field occurs. In fact, we expect this limit to have significant steady ion flux j^+ and the polarization is now determined by the steady Ohmic current.

5. High-Peclet theory

At large $Pe \sim O(\epsilon^{-1})$, tangential flux is no longer negligible in the diffusion layer. A thinner diffusion layer is also associated with large *Pe*. Its dimensionless thickness should scale as $Pe^{-1/2}$ due to the velocity slip and the uniform velocity profile within it. This thin electroneutral layer would prevent of the polarized layer to grow indefinitely. In essence, convection brings in an electroneutral solution to neutralize the polarized region and to stop dynamic charging before complete screening occurs.

We hence expect the length of the polarized region to be shorter. This weaker polarization (and the larger flux) allows (requires) more external field penetration and scaling (13) applies. With more external field leakage but less polarization, we expect from (16) the electrophoretic velocity to be less than Dukhin's scaling (2) at large *Pe*. Unlike the complete screening case, we need to resolve the polarized region to determine the polarization due to the steady Ohmic current.

The slip velocity $U_s(\theta)$ within this diffusion layer is the asymptotic limit of $u(y \to \infty)$ from the polarized region. From (16) and (22), we have

$$U_s(\theta) = -\zeta \left(\frac{\partial \Phi}{\partial \theta}\right)_0 - \Phi_0(\theta)\left(\frac{\partial \Phi}{\partial \theta}\right)_0. \tag{44}$$

A convenient tangential coordinate for this boundary layer is defined by the local stream line with the azimuthal single θ as its coordinate and its locally orthogonal coordinate represented by the stream function

$$\psi = (r-1)\sqrt{P} = y\sqrt{P}, \tag{45}$$

where

$$\sqrt{P}\,U_\theta = \frac{1}{\sin\theta}\frac{\partial \psi}{\partial y} \quad \text{and} \quad \sqrt{P}\,U_r = -\frac{1}{\sin\theta}\frac{\partial \psi}{\partial \theta}$$

for the axisymmetric three-dimensional flow field. With these coordinates (4) becomes

$$\frac{1}{U_s(\theta)\sin^2\theta}\frac{\partial C^\pm}{\partial \theta} = K^\pm \frac{\partial}{\partial \psi}\left(\pm C^\pm \frac{\partial \phi}{\partial \psi} + \frac{\partial C^\pm}{\partial \psi}\right). \tag{46}$$

Although *Pe* and *P* are not equivalent, we have used the original scaling with *P* to avoid introducing the unknown parameter *Pe*. However, all higher-order terms in Pe^{-1} have been omitted. Equation (46) can be further simplified with a new coordinate $\chi(\theta) = \int_0^\theta U_s(x)\sin^2 x\,dx$ representing a weighted running average of the slip velocity along the circumference. The value of χ starts at zero at the pole ($\theta = 0$) and increases toward the equator ($\theta = \pi/2$). With this new tangential coordinate, (38) becomes

$$\frac{\partial C^\pm}{\partial \chi} = K^\pm \frac{\partial}{\partial \psi}\left(\pm C^\pm \frac{\partial \phi}{\partial \psi} + \frac{\partial C^\pm}{\partial \psi}\right). \tag{47}$$

As for the classical diffusion boundary layer, (47) is amenable to a self-similar transform even though it contains an extra electromigration term. Using the self-similar variable $\eta = \psi/2\sqrt{\chi}$, (47) becomes an ordinary differential equation

$$-2\eta\frac{\partial C^\pm}{\partial \eta} = K^\pm \frac{\partial}{\partial \eta}\left(\pm C^\pm \frac{\partial \phi}{\partial \eta} + \frac{\partial C^\pm}{\partial \eta}\right). \tag{48}$$

We can now invoke the electroneutrality of the intermediate region, $C^- = C^+$. Adding the two equations in (48), we get a single ordinary differential equation

$$-2\eta\frac{\partial C}{\partial \eta} = \frac{\partial^2 C}{\partial \eta^2} \tag{49}$$

since $1/K^+ + 1/K^- = 2$. The solution of this equation is

$$C = 1 + A\frac{\sqrt{\pi}}{2}\big[\operatorname{erf}(\eta) - 1\big] \tag{50}$$

such that $C(\eta \to \infty) = 1$ to match with the Ohmic region.

Near the surface at $\eta = 0$, (50) simplifies to

$$C \sim 1 + A\eta - A\frac{\sqrt{\pi}}{2}. \tag{51}$$

Matching (51) to the intermediate asymptote (3.28) of the polarized region to account for the finite flux into the polarized region, we find the thickness of the high-*Pe* intermediate region is

$$y_* = \frac{1}{U_s \sin\theta}\sqrt{\frac{\pi\chi(\theta)}{P}}, \tag{52}$$

and it grows from zero at the pole toward the equator position D in Fig. 3.

The order of y_* is essentially $O(Pe^{-1/2})$, the boundary layer scaling. Hence, the scalings (12) and (13) which require the screening length $\beta = y_*^2/3\epsilon$ to be $O(\epsilon^0)$ or smaller

then requires *Pe* to be of $O(\epsilon^{-1})$. This limit is reached at very high fields. The field leakage is now significant such that $\partial\Phi/\partial r \sim O(\epsilon^0)$.

More explicitly, the coefficients for the effective external field conditions (35) are

$$\beta = \frac{\pi\chi(\theta)}{3P\epsilon U_s^2 \sin^2\theta}, \qquad V = \frac{1}{U_s \sin\theta}\sqrt{\frac{\pi\chi(\theta)}{P}}\frac{2}{3\epsilon}. \tag{53}$$

These coefficients are implicitly dependent on the slip-velocity $U_s = \frac{1}{2}(\partial\Phi^2/\partial\theta)(r=1)$ through $\chi(\theta)$. Hence the effective Ohmic electrostatic Laplace problem (8) must now be solved with a nonlinear differential–integral electrostatic slip condition. However, from the low-*Pe* result for the maximum Dukhin velocity $U_s(\theta)$ in (24), we do not expect U_s to depend strongly on θ. We hence approximate $U_s \sin\theta$ by $\langle U_s\rangle$, its average value, and also approximate χ by its mean value,

$$\chi \sim \langle U_s\rangle = \frac{2}{\pi}\int_0^{\pi/2} U_s\, d\theta. \tag{54}$$

This approximation simplifies (53) to

$$\beta = \frac{\pi}{3P\epsilon\langle U_s\rangle}, \qquad V = \sqrt{\frac{\pi}{P\langle U_s\rangle}}\frac{2}{3\epsilon}, \tag{55}$$

and hence provides a linear effective boundary condition for (35).

The solution of the Laplace equation with condition (35) and far-field condition $\nabla\Phi(r\to\infty) = -E_\infty \hat{e}_z$ can be readily solved. The external potential at the surface is

$$\Phi_0(\theta) = \Phi(r=1,\theta) = E_\infty \frac{3\beta}{1+2\beta}\cos\theta - V. \tag{56}$$

We neglect the first term in (44) and obtain the local slip velocity

$$\begin{aligned} U_s(\theta) &= \Phi(r=1,\theta) \\ &= \left(E_\infty \frac{3\beta}{1+2\beta}\cos\theta - V\right) E_\infty \frac{3\beta}{1+2\beta}\sin\theta. \end{aligned} \tag{57}$$

The average slip in dimensional variables is then

$$\begin{aligned} \langle U_s\rangle = {} & -E_\infty V \frac{6}{(3U_0\lambda\langle U_s\rangle/D + 2\pi)} \\ & + \frac{1}{\pi}\left(\frac{3E_\infty\pi}{3U_0\lambda\langle U_s\rangle/D + 2\pi}\right)^2. \end{aligned} \tag{58}$$

It is clear that the second term dominates and, to leading oder,

$$|U_e| = \frac{\bar{\pi}}{2}\langle U_s\rangle = \frac{1}{2}\left(\frac{3E_\infty\pi}{6U_0U_e\lambda/(D\pi) + 2\pi}\right)^2. \tag{59}$$

Hence, at low field and low electrophoretic velocity, we recover the $\bar{E}_\infty^2$ scaling of the nonlinear part of the low-*Pe* theory in (27). Even the coefficient agrees despite the uniform slip velocity assumption here. This suggests that a uniform theory can be formulated for both limits of *Pe*. In the limit of large velocity, a new scaling for U_e is obtained,

$$|U_e| = \frac{1}{2}\left(\frac{\pi^2 D}{U_0\lambda}\right)^{2/3} E_\infty^{2/3}, \tag{60}$$

or in dimensional form

$$|U_e| = \frac{1}{2}\left(\frac{\pi^2 D}{\lambda}\right)^{2/3}\left(\frac{\epsilon}{\mu}\right)^{1/3} E_\infty^{2/3} a^{1/3}. \tag{61}$$

Unlike Dukhin's screened slip velocity (27), this finite penetration slip velocity is dependent on the diffusivity and the electrolyte concentration.

Both (60) and (61) do not have the same dimensionless parameters as the low-*Pe* theory (27). They hence cannot be depicted in Fig. 4. However, the two sets of large U_e data in Fig. 4, which are not captured by the low-*Pe* scaling, have large particle diameters of 100 and 250 μm and have similar electrolyte concentrations. Using $a = 175$ μm as an average value and typical values of the other parameters stated in the caption of Fig. 4, we obtain $U_0 = 3.2\times10^{-4}$ cm/s and (60) becomes $U_e \sim 1.4\times10^3 \bar{E}_\infty^{2/3}$. This specific limit for $a = 175$ μm is plotted in Fig. 4. Both sets of data $a = 100$ and 250 μm are seen to approach this specific high-field limit. In all our correlations, the characteristic diffusivity used is $D = 2\times10^{-5}$ cm^2/s, the zeta potential $\zeta = 41$ mV, permittivity of water $\hat{\epsilon} = 6.9\times10^{-10}$ C2 N^{-1} m^{-2} and viscosity $\mu = 1.0$ cP.

Equation (60) offers the general scalings for any a that are realized at large radius and large electric field with $Pe \sim O(\epsilon^{-1})$. This scaling is equivalent to saying that the Debye layer Peclet number $U\lambda/D^+$ is of order unity $O(\epsilon^0)$. The tangential convection of ions in the polarized layer is still much weaker than the normal flux term. (The ratio of the two is $O(\epsilon U\lambda/D^+)$.) However, by controlling the flux of ions through the all-important diffusion layer and limiting the thickness of the polarized layer, tangential convection in the electroneutral diffusion layer has significantly enhanced the external field penetration and reduced the polarization to produce a weaker electrophoretic velocity. As seen in Fig. 4, the high-*Pe* data have yet to reach this limit. However, using (59) for both low and high *Pe*, we are able to satisfactorily collapse all data with E_∞ beyond $E_\infty \sim 20$ in Fig. 5. Correlation (59) is within a factor of 10 of all data in this range, and is within a factor of 2 of data by Mishchuk and Takhistov.

Correlation (59) seems to capture well the intermediate data at $E_\infty = 10$ to 100 in Fig. 4. However, the data beyond $E_\infty = 100$, with presumably much larger *Pe*, begin to deviate and exceed the prediction by a factor of 10. The term omitted in (60) has lowered the prediction significantly such that (60) overpredicts in Fig. 4 but underpredicts in Fig. 5.

There are several possible reasons why our theory underpredicts the measured velocity at high field. We have made several simplifications to arrive at a closed-form correlation, viz., uniform slip velocity and screening length. In reality, there could be stagnation points on the surface other than those at the pole and equator. At high *Pe* with

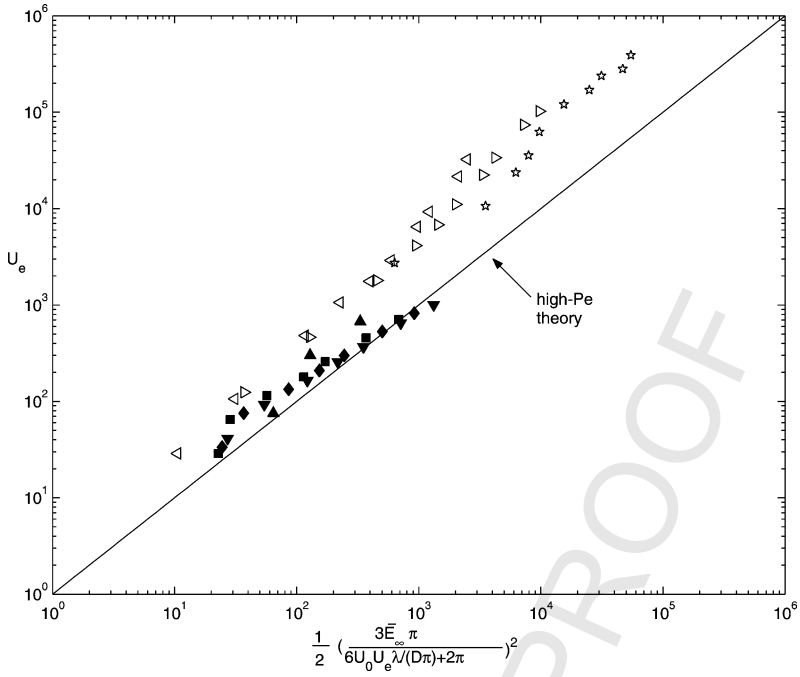

Fig. 5. Collapse of high-speed data with $\bar{E}_\infty > 20$ in Fig. 4. The x-axis is $\frac{1}{2}\left(\frac{3\bar{E}_\infty\pi}{6U_0\lambda\langle U_s\rangle/D+2\pi}\right)^2$, and the y-axis is U_e. The straight line is our theory of Eq. (59) valid for both low and high *Pe*. The symbols are identical to those in Fig. 4.

strong convection, charges could accumulate at those points to produce excess polarization. At the high fields necessary to reach large *Pe* (>100 V/cm), surface reactions can also occur at the granule to produce excess counterions. Nevertheless, it is quite clear from Figs. 4 and 5 that the breakdown of Dukhin's low-*Pe* scaling is due to the presence of a convection–diffusion boundary layer that stops the transient charging before complete screening occurs.

6. Discussion

The diffusion layer plays a key role in this current flux-induced nonlinear electrokinetics. At low Peclet numbers, the thick diffusion layer and the polarized layer produce complete steady-state screening. The polarization is hence due entirely to transient capacitative charging. Complete screening produces large tangential field and transient charging produces the largest polarization. In this case, we obtain Dukhin's scaling (2) for the maximum electrophoretic velocity.

At high Peclet numbers, the normal flux is enhanced by tangential convection due to electroosmotic flow. The thinness of the electroneutral convection–diffusion layer actually shortens transient charging before complete screening occurs. The polarization is induced by the steady Ohmic current due to the penetrating field. This allows more external field penetration and reduces polarization. The electrophoretic velocity is hence lower relative to the low-*Pe* value.

For both transient charging at low *Pe* and steady current at high *Pe* to be possible, the granule should be an isopotential body as well as one that is penetrable to the counterions that carry the current. An electrically insulated membrane would not result in significant polarization beyond that endowed by its bound surface charge.

The extended polarized region also holds as much charge as the external electromigration and diffusion fluxes allow it both during transient charing and steady current penetration. Its capacitance is not limited by the total bound surface charge.

These unique properties of this DC nonlinear electrokinetic phenomenon allows it to produce an electrokinetic mobility 100 times larger than its linear counterpart. Is nonuniform polarization also produces vortices on the side receiving the counterion flux [26].

Acknowledgments

This work is supported by an NSF-XYZ-on-a-Chip grant, a NASA grant, and the Notre Dame Center for Microfluidics and Medical Diagnostics. We are grateful to R. Zhou and P. Takhistov for measuring the data points indicated in Fig. 4.

References

[1] A.V. Delgado, Interfacial Electrokinetics and Electrophoresis, Marcel Dekker, 2002.
[2] R.F. Probstein, Physicochemical Hydrodynamics, Wiley–Interscience, 1994.

[3] F.A. Morrison Jr., J. Colloid Interface Sci. 34 (1970) 210.
[4] P. Takhistov, A. Indeikina, H.-C. Chang, Phys. Fluids 14 (2002) 1.
[5] R.W. O'Brien, L.R. White, J. Chem. Soc. Faraday Trans. 2 74 (1978) 1607.
[6] D. Dutta, D.T. Leighton, Anal. Chem. 74 (5) (2002) 1007.
[7] H.-C. Chang, The MEMS Handbook, CRC Press, 2001, 11-1.
[8] A. Ramos, A. González, A. Castellanos, N.G. Green, H. Morgan, Phys. Rev. E 67 (2003) 056302.
[9] H.A. Pohl, Dielectrophoresis, Cambridge Univ. Press, 1978.
[10] A. González, A. Ramos, N.G. Green, A. Castellanos, H. Morgan, Phys. Rev. E 61 (2000) 4019.
[11] T. Squires, M.Z. Bazant, preprint, 2004.
[12] A. Ajdari, Phys. Rev. E 61 (2000) R45.
[13] A.B.D. Brown, C.G. Smith, A.R. Rennie, Phys. Rev. E 63 (2000) 016305.
[14] Y. Solomentsev, M. Bohmer, J.L. Anderson, Langmuir 13 (1997) 6058.
[15] Y. Solomentsev, S.A. Guelcher, M. Bevan, J.L. Anderson, Langmuir 16 (2000) 9208.
[16] A.R. Minerick, R. Zhou, P. Takhistov, H.-C. Chang, Electrophoresis 24 (2003) 3703.
[17] M. Trau, D.A. Saville, I.A. Aksay, Langmuir 13 (1997) 6375.
[18] S.R. Yeh, M. Seul, B.I. Shraiman, Nature 386 (1997) 57.
[19] F. Nadal, F. Argoul, P. Hanusse, B. Pouligny, A. Adjari, Phys. Rev. E 64 (2002) 061409.
[20] Y. Hu, J.L. Glass, A.E. Griffith, J. Chem. Phys. 100 (6) (1994) 4674.
[21] S.K. Thamida, H.-C. Chang, Phys. Fluids 14 (2002) 4315.
[22] S.S. Dukhin, Adv. Colloid Interface Sci. 35 (1991) 173.
[23] N.A. Mishchuk, S.S. Dukhin, Interfacial Electrokinetics and Electrophoresis, Marcel Dekker, 2002.
[24] N.A. Mishchuk, P.V. Takhistov, Colloids Surf. A 95 (1995) 119.
[25] S. Barany, N.A. Mishchuk, D.C. Prieve, J. Colloid Interface Sci. 207 (1998) 240.
[26] Y. Ben, H.-C. Chang, J. Fluid Mech. 461 (2002) 229.